

LANDSCAPE PATTERN EVOLUTION AND ECOLOGICAL RISK DRIVING MECHANISMS IN A TRADITIONAL INDUSTRIAL CITY: EVIDENCE FROM ZHUZHOU, CHINA

YI, H. L.¹ – ZHU, J. J.^{2,3*}

¹*Department of Environmental Design, School of Packaging Design and Art, Hunan University of Technology, Zhuzhou 412007, China*

²*College of Horticulture and Forestry Sciences, Huazhong Agricultural University, Wuhan 430070, China*

³*Hubei Scientific Research Station for Integrated Land Consolidation and Rehabilitation in the Jiangnan Plain, Ministry of Natural Resources, Wuhan 430071, China*

*Corresponding author
e-mail: jjaji_zhu@163.com

(Received 14th Apr 2025; accepted 16th Jun 2025)

Abstract. Amid global urbanization, traditional industrial cities face increasingly complex ecological risks resulting from the interplay of industrial pollution and imbalanced land use patterns, leading to ecological security concerns. Therefore, assessing landscape ecological risk (LER) in traditional industrial cities and identifying its driving factors are crucial for safeguarding ecological security patterns and advancing sustainable urban development. Zhuzhou, one of China's first eight key industrial cities, has experienced intensive urban expansion and long-term industrial legacies, facing unique ecological vulnerabilities, and was therefore chosen as the study area. An ecological risk assessment model was constructed using land use data to analyze the spatiotemporal evolution of LER from 2000 to 2020. Additionally, the Geodetector model was employed to identify the driving factors on a regional scale. The findings indicate that (1) Zhuzhou's land use is primarily composed of woodland and arable land, with frequent conversions between the two. Over time, landscape fragmentation has intensified, while ecological protection policies have slightly improved landscape connectivity. (2) Low-risk and medium-low risk areas account for over 70%, while notably, medium-low and medium-high risk areas have significantly expanded in area. LER exhibits a significant positive spatial correlation, which has weakened over time. (3) More than 75% of the study area maintained stable LER levels. LER changes follow a dynamic pattern of core improvement and peripheral deterioration, yet the overall LER level has slightly increased, indicating a decline in ecosystem stability. (4) LER is primarily influenced by the normalized difference vegetation index (NDVI), elevation, and PM2.5 concentration. NDVI and elevation exhibited consistently high q-values in their interactions with other factors, and NDVI-related interactions played the most significant role in LER evolution. This study supports future ecological protection and risk management in Zhuzhou, while providing a scientific basis for ecological planning, sustainable land management, and risk control in similar cities worldwide.

Keywords: *landscape ecological risk (LER), land use patterns, landscape fragmentation, geodetector, PM2.5 pollution*

Introduction

Global industrialization and urbanization have accelerated population growth and economic expansion, particularly in developing countries. These transformations have accelerated land use/cover change (LUCC) processes (Xu et al., 2016; Liu et al., 2022). While land use sustains natural resources and ecosystem services, intensified human activities have reshaped land use patterns, causing habitat degradation and reduced these services, ultimately heightening ecological risks (Foley et al., 2005; Turner et al., 2007; Grimm et al., 2008; Albert et al., 2020; Xie et al., 2020). These changes pose severe

threats to human well-being and undermine the sustainability of natural ecosystems and socio-economic systems (Ran et al., 2022). To address these challenges, various countries have implemented proactive measures. For instance, Europe introduced the European Landscape Convention in 2000, promoting landscape conservation and management (Pătru-Stupariu and Nita, 2022). Since 2012, China has advocated for ecological civilization, emphasizing the dialectical unity between the environment and the economy (Hu, 2018). Unlike Europe's landscape conservation-oriented approach, China's ecological civilization strategy integrates ecological protection with socio-economic development, providing a comprehensive framework particularly relevant to rapidly industrializing regions. Additionally, the United Nations launched the 2030 Agenda for Sustainable Development in 2015, aiming to tackle global challenges (Lee et al., 2016).

Ecological risk denotes the adverse effects of external pressures on species' ecological functions, ecosystems, or landscapes, potentially leading to declines in ecosystem health, productivity, genetic diversity, economic value, and aesthetic appeal (Chen et al., 2013; Haque et al., 2022; How et al., 2023). Traditional ecological risk assessments have predominantly examined the toxicity of chemical pollutants and their effects on human health (Chen et al., 2006). However, with an expanding research scope, landscape ecological risk (LER) has emerged as a research hotspot due to its more comprehensive assessment framework (Cao et al., 2019). Unlike traditional assessment methods, LER places greater emphasis on regional spatiotemporal variations, scale effects, and the impact of landscape fragmentation on ecological risk (Chen et al., 2020). Recently, LER research has expanded to assess the cumulative impacts of multiple ecological risk sources on regional ecosystems, addressing increasingly complex ecological challenges (Mo et al., 2017; Rao et al., 2024). Accurate LER assessments underpin sustainable ecosystem management, contributing not only to the optimization of ecological conservation measures but also to enhancing human well-being and fostering balanced environmental and societal development (Harwell et al., 1992; Peng et al., 2023).

Conducting a thorough and precise assessment of LER is particularly challenging in areas with complex landscape patterns, where high diversity and uncertainty complicate the identification and quantification of risk sources. Landscape patterns, as products of the interactions between human activities and natural ecosystems, reflect variations in ecological processes and ecosystem structures. They serve as a critical tool for assessing habitat quality, biodiversity, LER, and broader ecological phenomena (Kadoya and Washitani, 2011; Fan et al., 2016; Chu et al., 2018). Different methods are employed in LER assessments depending on the characteristics of ecological risk sources. The source-sink-based approach is well-suited for regions where ecological risk sources are clearly defined (Malekmohammadi and Blouchi, 2014; Wu et al., 2021). In contrast, in regions with complex ecological risk sources and significant regional heterogeneity, landscape pattern-based assessment methods are more effective. While the former enables quantitative LER evaluation, its applicability is limited by complex and hard-to-access datasets. In contrast, the latter effectively describes how human disturbances and additional factors influence landscape structure, function, and processes within specific regions and assesses LER through a comprehensive multi-scale analysis. This approach overcomes the limitations of traditional assessment methods and offers greater applicability (Ji et al., 2021; Li et al., 2023). In recent years, landscape pattern-based LER assessment methods have been widely applied in multi-scale landscape ecological risk studies across various geographic regions and ecological functional areas. For example, research has been carried out at the national level (Zhang et al., 2022), in urban

agglomerations (Li et al., 2020; Shi et al., 2022; Wang et al., 2025), plateau regions (Hou et al., 2020), basins (Lin et al., 2020), river basins (Du et al., 2023), wetlands and lakes (Xie et al., 2021), and other ecologically fragile and functional zones (Gong et al., 2021; Tan et al., 2023). These studies provide important theoretical support for the further development and practical application of LER assessment methods.

Commonly used driving mechanism analysis methods include ordinary least squares (OLS) (Mondal et al., 2021), principal component analysis (PCA) (Aruhan and Liu, 2024), random forest regression (RFR) (Chang et al., 2023), geographically weighted regression (GWR) (Yuan et al., 2020; Li et al., 2022), support vector machine (SVM), artificial neural network (ANN) (Stupariu et al., 2022), Geodetector is also widely applied (Xu and Bao, 2022; Shi et al., 2023). Among these methods, Geodetector demonstrates notable advantages, particularly in identifying multiple driving factors and their interactions (Lu et al., 2023). It effectively reveals spatial variability and explains the factors and mechanisms contributing to such variability (Wang and Xu, 2017). Simultaneously, Geodetector does not require prior assumptions about the relationships between variables, making it particularly suitable for analyzing complex nonlinear relationships. It supports both quantitative and qualitative data, offering flexibility in handling multivariate data analysis. The applicability and effectiveness of the Geodetector method have been extensively validated across various research domains, including vegetation, climate, and environmental pollution studies (Wang et al., 2020; Zheng et al., 2021; Long et al., 2022).

In 2013, the Chinese government issued the National Old Industrial Base Adjustment and Transformation Plan (2013-2022), which included Zhuzhou City with the goal of addressing long-standing environmental pollution issues. The introduction of the Five-Year Action Plan for Chang-Zhu-Tan's Integrated Development (2021-2025) in Hunan Province, along with the establishment of the Chang-Zhu-Tan National Ecological Civilization Pilot Zone, has created new opportunities for the sustainable development of Zhuzhou City. The implementation of these policies has not only accelerated the systematic management of ecological issues but also provided strong support for Zhuzhou's ecological transition. As a typical traditional industrial city, Zhuzhou has long relied on heavy industry and manufacturing as its primary economic drivers. The imbalanced land use structure and concurrent development of industrialization have intensified resource consumption and pollution emissions, leading to landscape fragmentation, degradation of ecological functions, and significant threats to urban ecological security. Therefore, a scientific assessment of LER in traditional industrial cities has become an urgent research priority. Existing LER assessments have primarily focused on large-scale regions, such as suburban watersheds of major cities (Cheng et al., 2023), metropolitan areas (Zhang et al., 2024), and urban agglomerations (Deng et al., 2023; Zhuo et al., 2024). However, studies on small- and medium-sized cities—especially those with unique industrial backgrounds like Zhuzhou—remain limited. Zhuzhou's industrial legacy and ecological risk present distinct local characteristics in terms of geographical extent and human activity context. Its ecological restoration and risk management challenges differ significantly from those faced by large urban agglomerations, providing a unique perspective for ecological risk assessment. This study addresses the research gap in LER assessment for traditional industrial cities, identify the ecological challenges faced during their transition, and analyze the driving mechanisms underlying these risks. Furthermore, it seeks to optimize the ecological security

framework in traditional industrial cities while contribute to urban ecological transition and sustainable development.

Therefore, this study conducts a LER assessment of traditional industrial cities, using Zhuzhou as a case study, aiming to address the following key issues: (1) How has land use transformation occurred in Zhuzhou between 2000 and 2020, and how has it affected the landscape pattern? (2) How do the spatiotemporal differentiation patterns and levels of LER vary at the grid scale in response to land use type changes? (3) What are the key drivers of LER? Specifically, how do human activities and industrial pollution contribute to changes in LER?

Research materials and methods

Study area

Zhuzhou lies in eastern Hunan Province, positioned in the lower reaches of the Xiangjiang River, is one of China's first eight key old industrial bases. The study area encompasses the municipal districts of Zhuzhou—Hetang, Lusong, Shifeng, Tianyuan, and Lukou—covering approximately 1,917 km². The area is primarily hilly, with higher terrain on the periphery and open mountain basins and alluvial terraces in the center. It features abundant heat, ample sunlight, and high rainfall (*Fig. 1*). The urban districts of Zhuzhou represent the most concentrated area of industrialization, where land use changes, ecological risks, and pollution emissions are most prominent. To maintain analytical relevance, this study excludes lower-level counties. Specifically, Liling City, You County, Chaling County, and Yanling County were excluded because they are predominantly agricultural with relatively low levels of industrial development and limited data availability, which does not align with the study's focus on industrial ecological risks in urbanized areas.

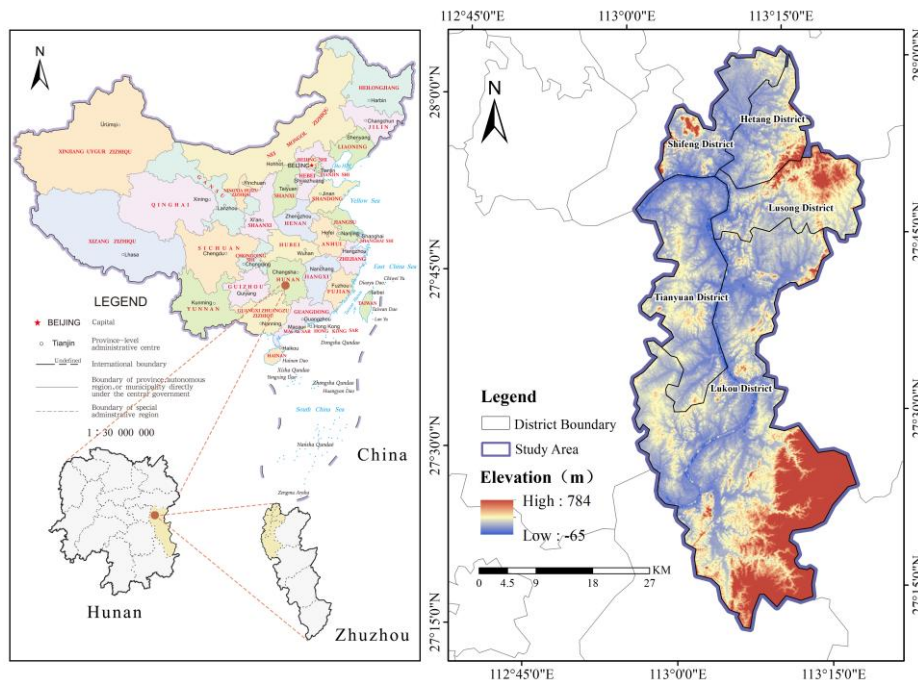


Figure 1. Study area map of Zhuzhou City

Data and sources

Land use data for five years (2000, 2005, 2010, 2015, and 2020) were obtained from the China Annual Land Cover Dataset (Yang and Huang, 2021). Based on research requirements, Land use was classified into arable land, woodland, grassland, water, construction land, and unused land. Elevation data were sourced from Geospatial Data Cloud (www.gscloud.cn), while slope were derived from it. The NDVI and GDP data were sourced from the Resource and Environmental Science and Data Center of the Chinese Academy of Sciences (<https://www.resdc.cn>). Annual precipitation and average annual temperature data were retrieved from the National Tibetan Plateau Science Data Center (<https://data.tpdc.ac.cn/home>). Road data were accessed from OpenStreetMap (www.openstreetmap.org), and Euclidean distance analysis was applied to calculate distance-based variables. Population density data were retrieved from WorldPop (<https://www.worldpop.org/>), while the nighttime light data were sourced from the National Earth System Science Data Center (<http://www.geodata.cn>). PM_{2.5} data were obtained from the China High Air Pollutants (CHAP) dataset (Wei et al., 2021). The distribution density of key emission enterprises was retrieved from the National Key Pollution Source Monitoring Database (<https://wryjc.cnemc.cn/>), and kernel density analysis was applied to assess spatial distribution characteristics. Additionally, sulfur dioxide (SO₂) emission data were selected from the Global Atmospheric Emissions Database (https://edgar.jrc.ec.europa.eu/dataset_ghg80).

Research methods

This study's framework comprises four key components. First, based on CLCD data, land use changes and landscape pattern dynamics are examined. Second, the LER assessment model is developed, and the landscape ecological risk index (ERI) is calculated to analyze the spatiotemporal evolution patterns and trends of LER. Third, spatial autocorrelation analysis is performed to identify LER clustering characteristics. Finally, Geodetector analysis is employed to identify key driving factors influencing LER and to assess the impacts of natural environmental conditions, regional accessibility, human activities, and pollution on ecological risk (Fig. 2).

Dynamic degree model

The single land use dynamic index quantifies the temporal change rate of a specific land use type. The formula is presented as follows:

$$K = \frac{U_b - U_a}{U_a} \times \frac{1}{T} \times 100\% \quad (\text{Eq.1})$$

where: K represents the change rate; U_a and U_b denote its area (km²) at the beginning and end of the period, respectively, while T indicates the duration (a).

The comprehensive land use dynamic index quantifies the overall intensity of land use change processes. The formula is presented as follows:

$$L_C = \frac{\sum_{i=1}^n \Delta L_{i-j}}{2 \sum_{i=1}^n U_i} \times \frac{1}{T} \times 100\% \quad (\text{Eq.2})$$

where: L_C represents the comprehensive land use dynamics area over a given time period; ΔL_{i-j} denotes the absolute area change between the start and end of time period,

representing the transition from land use type i to j ($i \neq j$); U_i represents the area of land use type i at the beginning of the period, while T indicates its duration.

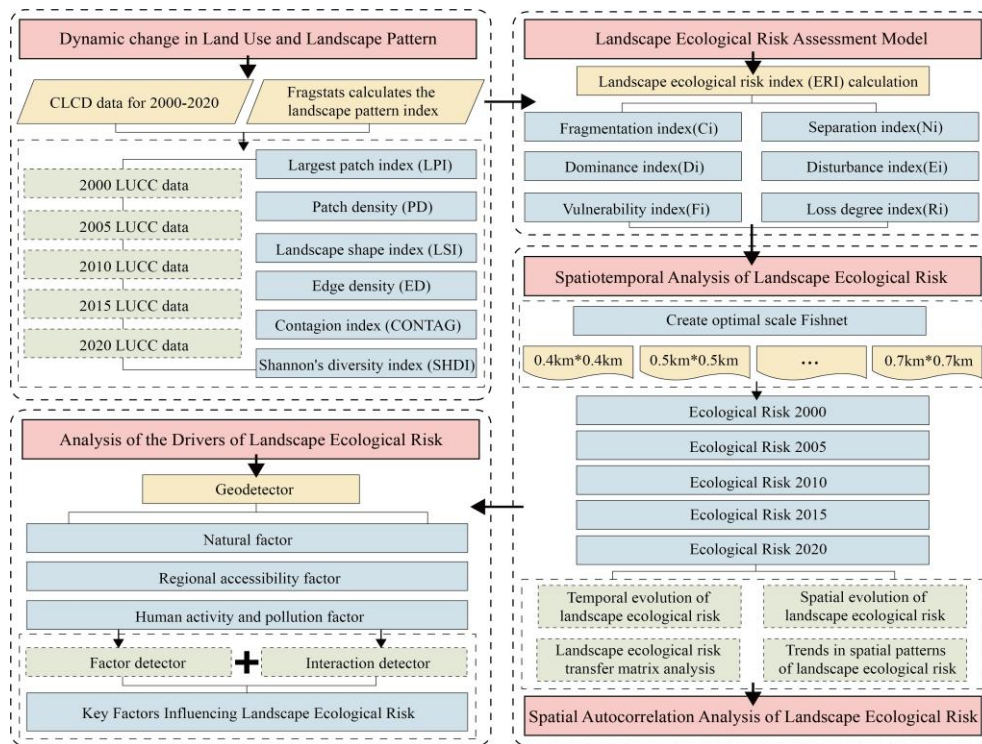


Figure 2. Study framework

Landscape pattern index

The landscape pattern index characterizes spatial structure and quantifies its relationship with ecological processes and spatial patterns. It facilitates a deeper understanding of landscape functions and is widely applied in quantifying landscape fragmentation, landscape heterogeneity, and spatial complexity. As a key method in landscape ecology, it is essential for quantifying spatial patterns. To examine the spatiotemporal characteristics of landscape change in Zhuzhou City and assess the evolution of different landscape types, this study selected six landscape indices at both the class and landscape levels. Among them, three class-level indices include largest patch index (LPI), patch density (PD), and landscape shape index (LSI), while three landscape-level indices include edge density (ED), contagion index (CONTAG), and Shannon diversity index (SHDI). The formulas for calculating these landscape indices are derived from the internal documentation of Fragstats 4.2.

LER assessment model

Risk Plot Division: Based on relevant studies, the size of a LER evaluation unit should be 2 to 5 times the average patch area (Yang et al., 2023). Given the relatively small extent of the study area, a grid size of 0.7 km × 0.7 km was selected. After removing grid cells whose center points were located outside the study area, in total, 4,197 evaluation units were identified. The final grid area was calculated to be approximately 4.8 times the average patch area, satisfying the standard criteria for risk unit division.

Calculation of ERI: The ERI was computed using landscape fragmentation, separation, and dominance, with the landscape loss index incorporated into the risk assessment framework. The final ERI values were calculated in Excel, following the methodology outlined in *Table 1*.

Table 1. Formulas and significance of landscape ecological risk index

Index name	Formula	Index significance
Landscape fragmentation index(C_i)	$C_i = \frac{n_i}{A_i} D_i$ (Eq.3)	The complexity of spatial distribution of landscape types after encountering external disturbances. n_i represents the number of patches for landscape type i ; A_i denotes the area of landscape type i .
Landscape separation index(N_i)	$N_i = \frac{1}{2} \sqrt{\frac{n_i}{A_i}} + \frac{A}{A_i}$ (Eq.4)	The level of patch heterogeneity within a given landscape. A represents the total area of all the landscapes.
Landscape dominance index(D_i)	$D_i = \frac{(Q_i+M_i)}{4} + \frac{L_i}{2}$ (Eq.5)	Significance of a given patch type within the landscape. Q_i represents the proportion of the grids containing patch i relative to the total number of grids; M_i denotes the proportion of patch i relative to the total number of patches; L_i indicates the proportion of the area of patch i to the total sample area.
Landscape disturbance index(E_i)	$E_i = aC_i + bN_i + cD_i$ (Eq.6)	The degree of anthropogenic disturbance to the landscape. The weighting coefficients satisfy $a+b+c=1$, where $a=0.5$, $b=0.3$, and $c=0.2$, respectively.
Landscape vulnerability index(F_i)	F_i (Eq.7)	Sensitivity, vulnerability, and resistance to external disturbances. The expert scoring method was adopted and then normalized. Water = 6, Unused land = 5, Arable land = 4, Grassland = 3, Woodland = 2, Construction land = 1.
Landscape loss degree index(R_i)	$R_i = \sqrt{E_i \times F_i}$ (Eq.8)	Ecological losses caused by external disturbances. Higher values indicate stronger disturbance. All other variables are defined as in previous equations unless otherwise noted.

The ERI reflects spatiotemporal variations in ecological conditions (Wang et al., 2021), and its formula is presented as follows:

$$ERI_i = \sum_{k=1}^N \frac{A_{ki}}{A_k} R_i \quad (\text{Eq.9})$$

where: ERI_i represents the ecological risk index of the i th risk unit, A_{ki} denotes the area of landscape type i within the k th risk unit, while A_k indicates its total area.

Based on the calculation results, Kriging interpolation was applied to spatially analyze the LER of each risk unit and to explore its spatial evolution characteristics. Kriging interpolation is based on the spatial semivariance function, which enables the estimation of risk values at unobserved locations (Setiyoko et al., 2020). Currently, there is no standardized classification for LER. To facilitate time-series comparisons, this study adopts the natural breaks method to classify ERI into five levels, using the 2000 ERI as the baseline (Liu et al., 2019). The risk indices for subsequent years were classified consistently based on the 2000 standard (*Table 2*).

Table 2. Classification of LER levels

Risk level	ERI value range
Low	0.3144–0.3721
Medium-low	0.3721–0.4535
Medium	0.4535–0.6419
Medium-high	0.6419–0.9493
High	0.9493–2.2638

Spatial analysis model

Spatial autocorrelation analysis is applied to examine the spatial dependence among LER values in adjacent evaluation units. This study employs Global and Local Moran's I to evaluate the spatial clustering of LER (Ke et al., 2021).

The Global Moran's I quantifies overall spatial autocorrelation of risk values, ranging from -1 to 1. > 0 signifies a positive correlation, = 0 signifies no correlation, < 0 signifies a negative correlation. Local Moran's I, in contrast, measures spatial heterogeneity within the study area. A positive value (> 0) suggests high-high or low-low clustering, while a negative value (< 0) indicates high-low or low-high clustering. The formula is presented as follows:

$$\text{Global Moran's } I = \frac{n \sum_{i=1}^n \sum_{j=1}^n w_{ij} (x_i - \bar{x})(x_j - \bar{x})}{\sum_{i=1}^n \sum_{j=1}^n w_{ij} \sum_{i=1}^n (x_i - \bar{x})^2} \quad (\text{Eq.10})$$

$$\text{Local Moran's } I = Z_i \sum_{j=1}^n w_{ij} Z_j (i \neq j) \quad (\text{Eq.11})$$

where: n denotes the total number of risk evaluation units, x_i and x_j are the LER values of evaluation units i and j , respectively, \bar{x} represents the mean LER value, Z_i and Z_j are the standardized risk values of evaluation units i and j , respectively, w_{ij} is the spatial weight matrix.

Geodetector model

Grounded in the principle of spatial heterogeneity, Geodetector identifies the major driving factors of LER by detecting spatial regional heterogeneity and spatial hierarchical heterogeneity. The core idea is that if the spatial distribution of a factor exhibits significant similarity to LER, that factor exerts a significant impact on ecological risk, thereby revealing the driving relationship between the factor and LER (Lu et al., 2023). Factor detection assesses each factor's explanatory power in the spatial variability of LER. Interaction detection evaluates the extent to which the interaction between two factors influences changes in ecological risk.

Considering the geographic characteristics and socioeconomic development of the study area, the influencing factors were categorized into three main groups based on their characteristics: natural factors, regional accessibility factors, human activities and pollution factors. Natural factors consist of elevation (X1), slope (X2), NDVI (X3), annual average temperature (X4), and annual precipitation (X5). Human activities and pollution factors include population density (X6), PM_{2.5} concentration (X7), Nighttime light (X8), GDP (X10), distribution density of key polluting enterprise (X11), and SO₂

emission (X12). Regional accessibility factors include Distance to road (X9). All factors were grouped into nine categories using the natural breaks method and converted into categorical variables for analysis. Further methodological details can be found in relevant literature (Wang and Xu, 2017).

Result and analysis

Spatiotemporal changes in land use

As illustrated in Fig. 3, Arable land is primarily distributed in the central and southern regions along the Xiangjiang River and its tributaries, exhibiting a strong correlation with the transportation network. Woodland covers most of the study area, particularly in mountainous and hilly regions. Water, apart from the Xiangjiang River, is also scattered in arable land and peri-urban areas. Construction land is predominantly distributed in and around urban centers in the northern and central regions, particularly at the interfaces between water and arable land. Grassland and unused land cover a comparatively small area, with insignificant changes in distribution.

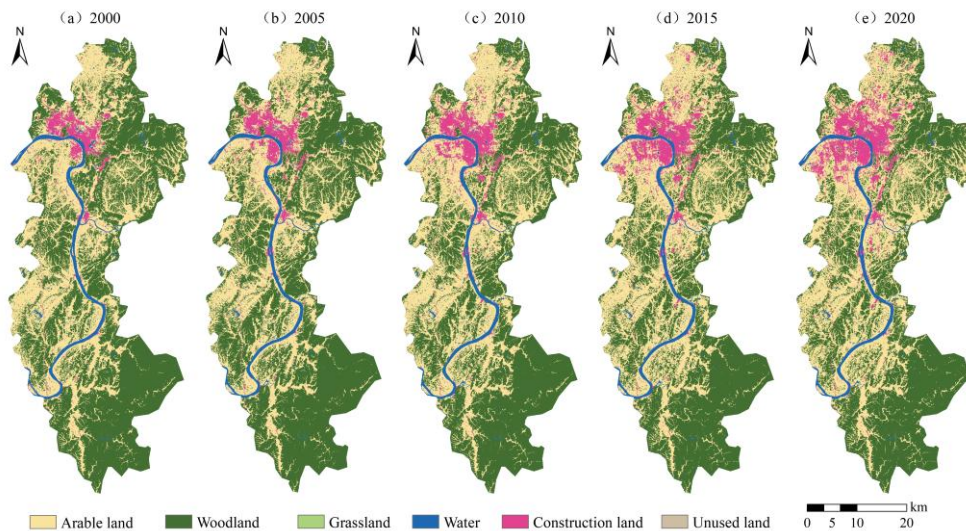


Figure 3. Land use distribution in the study area (Zhuzhou City, 2000–2020)

Between 2000 and 2020, arable land and construction land expanded continuously, whereas woodland, grassland, and water showed a declining trend (Table 3). The arable land area increased from 740.73 km² to 787.79 km², a 6.35% increase, particularly between 2005 and 2010. By 2020, arable land constituted 41.08% of the total area. The woodland area decreased from 1,041.14 km² to 909.50 km², a 12.64% reduction, with the most notable change occurring between 2010 and 2015, when its proportion dropped from 50.11% to 47.66%. Grassland area also decreased significantly, from 1.09 km² to 0.86 km², a 20.61% decline, especially between 2005 and 2010. Water exhibited slight fluctuations, decreasing from 69.48 km² in 2000 to 68.03 km² in 2020, a 2.08% reduction. Construction land underwent the most substantial expansion, increasing from 65.43 km² to 151.70 km², a 131.86% increase. Unused land remained relatively stable, with only 0.01 km² recorded in 2020 (Table 3).

Table 3. Land use structure of the study area (Zhuzhou City, 2000–2020)

Land Type	Area (km ²), Ratio (%)									
	2000		2005		2010		2015		2020	
	Area	Ratio	Area	Ratio	Area	Ratio	Area	Ratio	Area	Ratio
Arable land	740.73	38.62	700.00	36.50	782.12	40.78	805.48	42.00	787.79	41.08
Woodland	1041.14	54.28	1067.31	55.65	960.98	50.11	914.02	47.66	909.50	47.42
Grassland	1.09	0.06	0.91	0.05	0.89	0.05	0.88	0.05	0.86	0.04
Water	69.48	3.62	70.03	3.65	70.32	3.67	70.32	3.67	68.03	3.55
Construction land	65.43	3.41	79.66	4.15	103.61	5.40	127.21	6.63	151.70	7.91
Unused land	0.04		0.00		0.00		0.00		0.01	

According to *Table 4*, the fluctuation in the dynamic change of construction land was the most significant, reaching 6.01% during 2005–2010, representing the most dramatic shift within the five study periods. The dynamic change rate of woodland exhibited a continuous negative trend, starting at -0.50% during 2000–2005 and remaining negative from 2005 to 2020. Arable land experienced complex fluctuations: It declined by -1.10% during 2000–2005, rebounded to 2.35% during 2005–2010, then fluctuated at 0.60% and -0.44% during 2010–2015 and 2015–2020, respectively. The dynamic change rate of grassland remained consistently negative, with the most notable decreases of -3.31% and -0.48% during 2000–2005 and 2005–2010, respectively. The fluctuation in water was relatively minor, ranging between 0.16% and -0.65% throughout the study period. Unused land showed minimal variation over time.

Table 4. Land use dynamics of the study area (Zhuzhou City, 2000–2020)

Land Type	Land Use Dynamics (%)			
	2000–2005	2005–2010	2010–2015	2015–2020
Arable land	-1.10	2.35	0.60	-0.44
Woodland	0.50	-1.99	-0.98	-0.10
Grassland	-3.31	-0.48	-0.22	-0.29
Water	0.16	0.08	0.00	-0.65
Construction land	4.35	6.01	4.56	3.85
Unused land	-20.00	0.00	0.00	0.00
Combined land-use dynamics(%)	0.59	0.39	0.34	0.31

A chord diagram was generated to depict land use transfer relationships (*Fig. 4*). According to 2000–2020 data, bidirectional conversions primarily occurred between woodland and arable land, while exchanges among other land types were relatively limited. Woodland experienced the largest transfer-out area, totalling 177.54 km², mainly converted into arable land (156.58 km²) and construction land (20.85 km²). Arable land had a total transfer-out area of 114.81 km², primarily shifting to woodland (45.63 km²) and construction land (63.77 km²). Water was primarily transformed into arable and construction land, whereas grassland, construction land, and unused land exhibited smaller transfer-out areas.

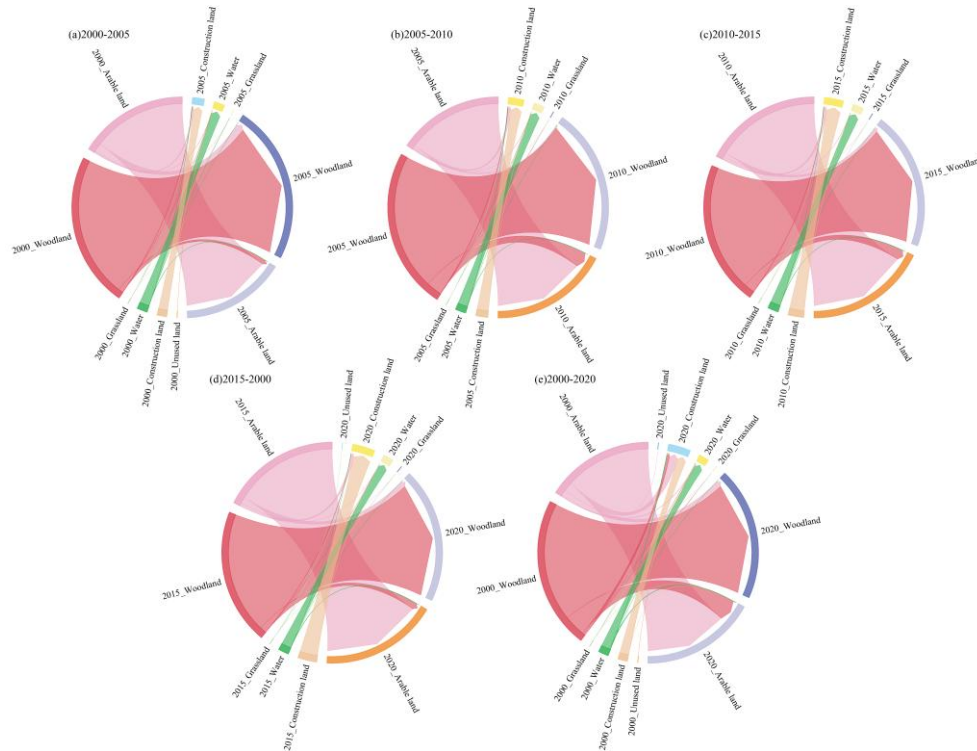


Figure 4. Land use transfer chord diagram in the study area (Zhuzhou City, 2000–2020)

The period 2005–2010 witnessed the highest total land use transfer within the study period, with 147.89 km² of land undergoing conversion. During this period, 114.17 km² of woodland was lost, primarily converted into arable land (110.53 km²). In contrast, during 2000–2005, arable land experienced the largest loss, with 74.47 km² being converted, mainly to woodland (60.33 km²). Between 2015 and 2020, the most significant expansion of construction land was recorded, increasing by 24.74 km², primarily from the conversion of arable land (22.49 km²).

Changes in landscape indices

At the class level (Fig. 5), the PD of arable land decreased from 4.1193 in 2000 to 3.1063 in 2020, indicating a gradual reduction in fragmentation and a trend toward a more concentrated and intensive landscape. In contrast, the PD of woodland increased from 2.7724 to 3.5173 between 2000 and 2015, and although it slightly declined to 3.0802 in 2020, the overall trend suggests a moderate increase in woodland fragmentation. Meanwhile, the PD of construction land increased from 1.6149 to 1.9133, indicating a progressive rise in fragmentation. The LPI of arable land increased steadily from 9.2129 in 2000 to 14.3256 in 2020, signifying an enhanced dominance of large arable land patches, with continuity improving year by year. The LPI of water declined between 2005 and 2010 but rebounded between 2015 and 2020, suggesting that water bodies faced a temporary decline during urbanization, but with the reinforcement of ecological protection efforts, water restoration has been achieved. A particularly notable change occurred in the LPI of construction land, which surged from 1.802 to 5.051, reflecting the expansion of construction land and an increasing clustering effect within the landscape. The LSI of arable land fluctuated considerably between 2000 and 2020, indicating an

irregular landscape pattern with high patch fragmentation. Meanwhile, the LSI of woodland remained relatively stable, reflecting a more regular landscape structure with minimal change. The LSI of water declined significantly from 34.0701 to 29.7127, indicating that water bodies have adopted a more regular shape with reduced edge complexity. In recent years, watershed protection policies and wetland restoration projects played a key role in reducing water landscape fragmentation. The LSI of construction land continuously increased from 50.2593 to 64.2579, suggesting that the morphology of construction land has become increasingly complex, with more irregular edge shapes, further exacerbating landscape heterogeneity.

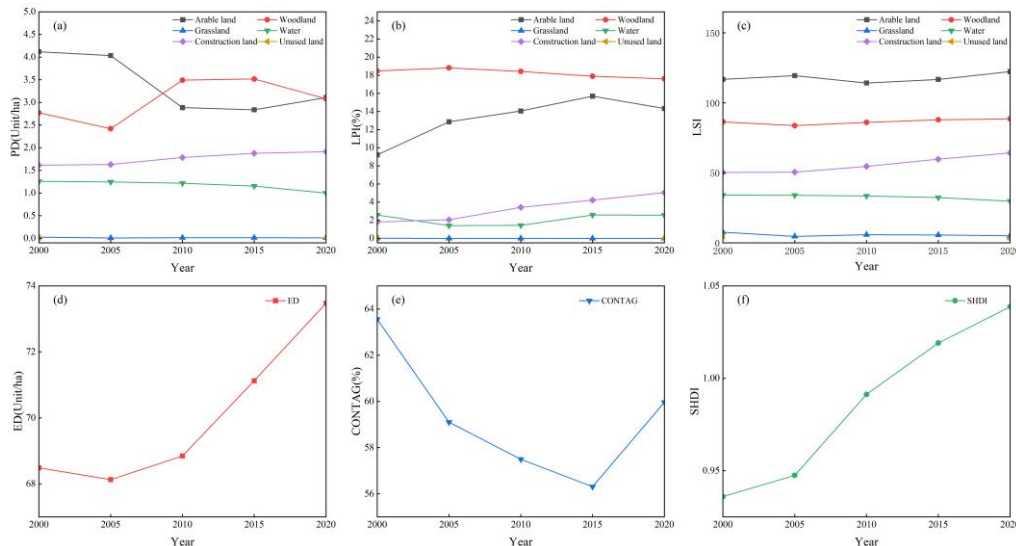


Figure 5. Trends in landscape pattern indices in the study area (Zhuzhou City, 2000–2020)

At the landscape level, ED increased year by year, rising from 68.4879 in 2000 to 73.472 in 2020, indicating a gradual increase in landscape fragmentation. This trend was particularly evident during urban expansion, where the growth of construction land increased patch edge areas, leading to a more complex landscape morphology. Conversely, CONTAG declined from 63.5535 in 2000 to 56.3102 in 2015, suggesting that landscape connectivity weakened over time. However, the index rebounded to 59.962 in 2020. Initiatives such as the construction of ecological corridors, green space planning, and urban greening projects have improved landscape connectivity. Meanwhile, SHDI steadily increased, rising from 0.936 in 2000 to 1.0387 in 2020, indicating greater landscape diversity and ecosystem complexity, as well as an overall increase in landscape richness.

Spatiotemporal variation analysis of LER

Spatial and temporal differentiation of LER

Between 2000 and 2010, the low-risk area occupied the largest share of the study area, comprising 44.26%, 45.59%, and 39.29%, respectively. However, in 2015–2020, the medium-low risk area became the dominant category, covering 41.84% and 41.64%, respectively. Overall, the medium-low risk area exhibited the most significant expansion, increasing by 192.90 km², followed by the medium-high risk area, which increased by

41.20 km². Meanwhile, the low-risk area underwent the most substantial decline, shrinking from 848.44 km² to 650.31 km², a reduction of 198.13 km². The high-risk and medium-risk areas also declined by 27.58 km² and 8.39 km², respectively (Table 5, Fig. 6).

Table 5. Area and ratio of LER levels in the study area (Zhuzhou City, 2000–2020)

Risk Level	Area (km ²), Ratio (%)									
	2000		2005		2010		2015		2020	
	Area	Ratio	Area	Ratio	Area	Ratio	Area	Ratio	Area	Ratio
Low	848.44	44.26	873.94	45.59	753.27	39.29	668.30	34.86	650.31	33.92
Medium-low	605.29	31.57	543.55	28.35	710.87	37.08	802.13	41.84	798.19	41.64
Medium	306.25	15.97	333.36	17.39	279.85	14.60	269.38	14.05	297.86	15.54
Medium-high	82.71	4.31	102.27	5.33	123.34	6.43	131.44	6.86	123.91	6.46
High	74.40	3.88	63.97	3.34	49.76	2.60	45.84	2.39	46.82	2.44

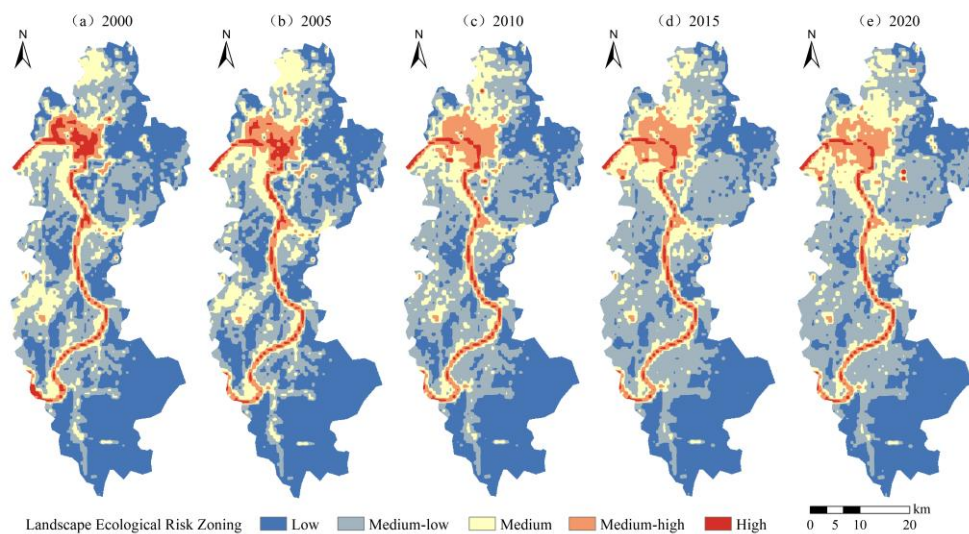


Figure 6. Spatial distribution of LER levels in the study area (Zhuzhou City, 2000–2020)

From 2000 to 2020, high-risk zones were predominantly concentrated in the city center, particularly at the intersection of Tianyuan, Shifeng, Hetang, and Lusong Districts, as well as in parts of the Xiangjiang River Basin and Lukou District. Over time, the high-risk zones gradually expanded outward from the urban core, but the overall ecological risk level exhibited a declining trend. Medium-high risk zones were primarily distributed in the city center and its periphery, progressively expanding into suburban areas at the urban fringe. In Shifeng District, the medium-high risk zones initially expanded northwestward before contracting, whereas in Tianyuan District, they continued to cluster southwestward (Fig. 6). The distribution of medium-risk zones gradually became more concentrated in the northern region, with a notable increase around urban areas after 2010. This reflects the urbanization process, which intensified ecological and environmental risks in these regions. Although the spatial extent of medium-risk zones remained relatively stable, their distribution gradually expanded from urban centers to peripheral

areas. Low-risk zones were closely associated with medium-low risk zones, predominantly distributed in the northern and southern mountainous areas, remote suburban regions of Zhuzhou, and nature reserves located far from urban centers. The ecological conditions in these areas were relatively stable, with minimal human disturbance. However, with urban expansion, some former low-risk zones gradually transitioned into medium-low risk zones, particularly in the central and mountainous regions of the study area (Fig. 6).

The LER levels demonstrated a clear transfer trend (Fig. 7). Low-risk areas were primarily converted into medium-low risk areas, with a transfer of 188.75 km². Medium-low risk areas expanded significantly, mainly shifting to medium-risk areas, with a transfer of 80.18 km². Medium-risk areas showed an overall decline, with 98.86 km² transitioning to medium-low risk and 19.89 km² shifting to medium-high risk, indicating that medium-risk areas were being redistributed toward both lower and higher risk categories. Medium-high risk areas primarily shifted to medium risk, while high-risk areas were predominantly converted into medium-high risk, with a transfer of 30.11 km². Overall, the LER structure in Zhuzhou City exhibited a trend toward concentration, with noticeable expansion of both medium-low and medium-high risk areas.

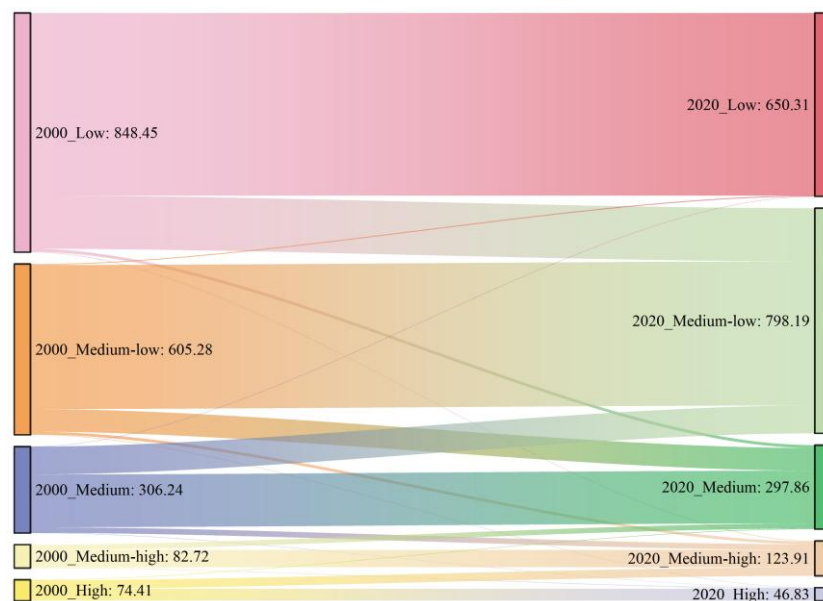


Figure 7. Conversion of LER areas by level in the study area (Zhuzhou City, 2000–2020)

Trend of LER change

The LER levels in the study area underwent pronounced changes, with distinct characteristics at each stage (Table 6, Fig. 8). Between 2000 and 2005, the total area experiencing LER changes was 165.56 km². The area of decrease covered 80.52 km², accounting for 4.20%, while the increased area reached 85.04 km² (4.44%), indicating that risk fluctuations were primarily localized. Areas with increasing risk were primarily in northern Tianyuan District and western Lusong District, with sporadic occurrences in the northern regions of the study area, though within a limited range. During 2005-2010, the area of increasing risk expanded to 173.28 km² (9.04%), significantly exceeding the decreased-risk area of 112.48 km². This period marked a notable deterioration in

ecological risk, with high-risk areas expanding sharply, particularly in the central and southwestern regions. Between 2010 and 2015, the extent of increasing risk declined, accounting for 6.85%. These areas were primarily distributed across the eastern, western, and southern regions of the study area, with sporadic occurrences along the Xiangjiang River and in the northern Shifeng District. Meanwhile, the distribution of decreasing risk remained limited and scattered, reflecting ongoing localized environmental degradation. From 2015 to 2020, LER stability improved significantly, with stable areas covering 93.76%. The percentage of decreasing and increasing risk areas declined to 2.31% and 3.93%, respectively.

Table 6. Areas and ratio of LER change trends in the study area (Zhuzhou City, 2000–2020)

Change Trends	Area (km ²), Ratio (%)									
	2000–2005		2005–2010		2010–2015		2015–2020		2000–2020	
	Area	Ratio	Area	Ratio	Area	Ratio	Area	Ratio	Area	Ratio
Decrease	80.52	4.20	112.48	5.87	56.80	2.96	44.34	2.31	152.55	7.96
Stable	1751.53	91.36	1631.33	85.09	1728.90	90.18	1797.50	93.76	1448.79	75.57
Increase	85.04	4.44	173.28	9.04	131.40	6.85	75.26	3.93	315.76	16.47

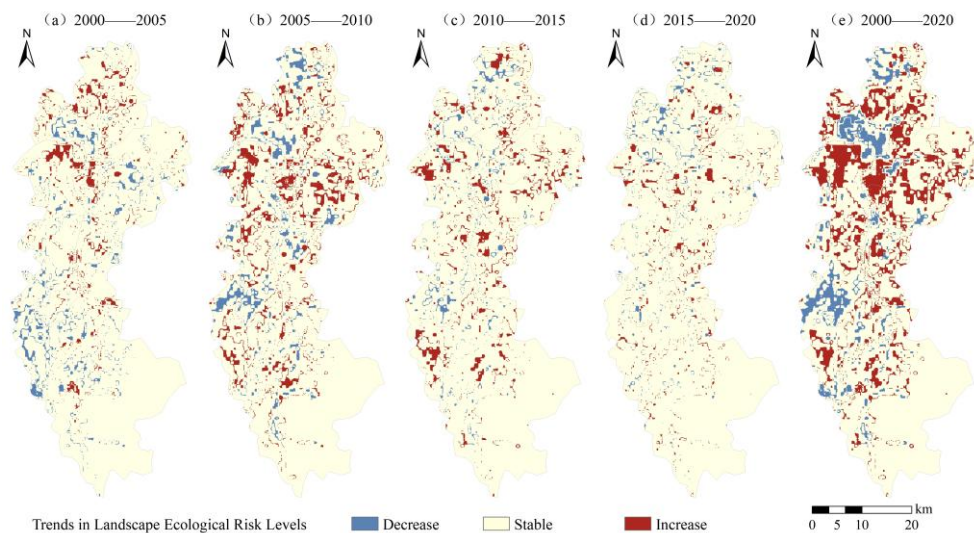


Figure 8. Change trends in LER levels in the study area (Zhuzhou City, 2000–2020)

Overall, from 2000 to 2020, the area experiencing changes in LER was smaller than the unchanged area (Table 6, Fig. 8), indicating a dynamic pattern of “core improvement and peripheral deterioration.” The risk decrease zones were primarily in the urban center, southwestern Tianyuan District, and northern Shifeng District, where ecosystem stability gradually improved due to the significant effects of corridor construction and natural ecological restoration. Conversely, the zones of increasing risk were mainly in the cores of Tianyuan and Lusong Districts, along with parts of Hetang and Lukou Districts. These zones were strongly influenced by industrialization and urbanization, where high-intensity human activities have led to drastic land use changes and a decline in vegetation cover, further exacerbating ecosystem instability.

Spatial autocorrelation analysis of LER

From 2000 to 2020, the global Moran's I value in the study area showed an overall declining trend, while maintaining a high level of spatial autocorrelation (*Fig. 9*). For the five periods, the global Moran's I values were 0.685, 0.686, 0.662, 0.650, and 0.621, respectively, with P-values < 0.001, indicating that the distribution of LER significantly positive spatial and a correlated clustered distribution pattern. However, the overall spatial correlation has weakened over time.

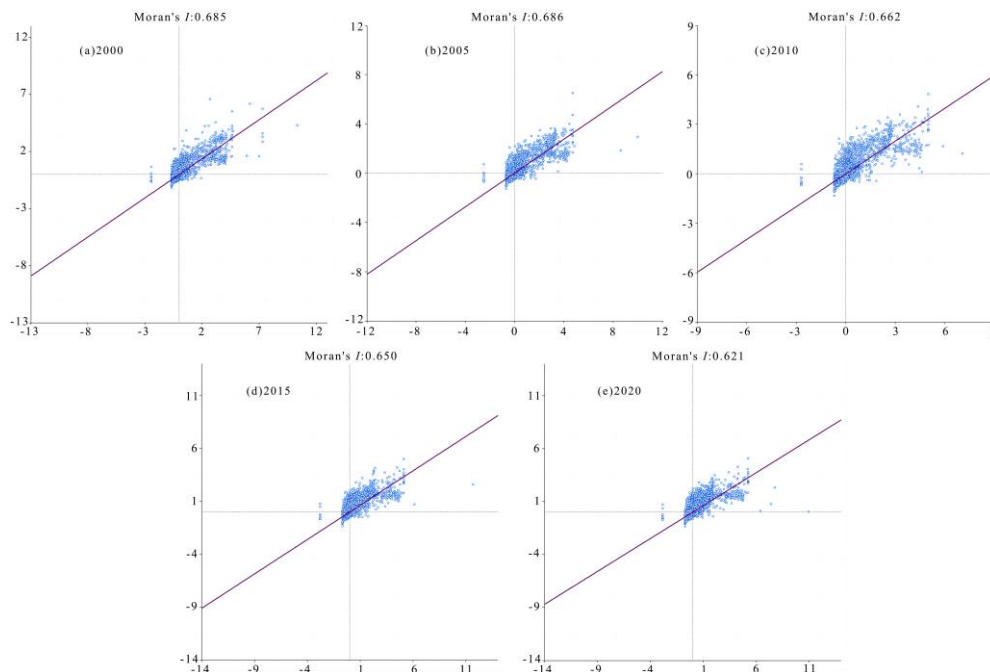


Figure 9. Scatterplots of Moran's I for LER in the study area (Zhuzhou City, 2000–2020)

According to *Fig. 10*, both "High-High" and "Low-Low" risk clusters expanded. In 2000, the "High-High" risk clusters consisted of 501 grid cells, while the "Low-Low" risk clusters covered 1,192 grid cells. By 2020, these figures increased to 611 and 1,201 grid cells, respectively. The "High-High" risk zones were primarily concentrated in the city center and along the Xiangjiang River, which are key areas for future risk control and ecological restoration. The "Low-Low" risk zones were predominantly located along the study area's northern and southern edges. However, their extent has gradually decreased since 2005, reflecting a potential expansion of ecological risks or insufficient protection measures. Additionally, the "High-Low" and "Low-High" heterogeneous clusters exhibited limited change and remained scattered. Overall, although high-risk core zones are well-defined in spatial distribution, the dynamic changes in low-risk zones and the potential risks associated with heterogeneous clusters require further attention to effectively mitigate the spread and evolution of ecological risks.

Analysis of drivers of LER evolution

Single factor detection

From 2000 to 2020, NDVI exhibited the most substantial explanatory power among natural factors for LER evolution in the study area, contributing 29.08%, 26.58%,

22.15%, 26.72%, and 21.73% across the five periods (Table 7). Over time, vegetation degradation has progressively intensified ecological risk. The influence of elevation on LER has also grown, with its contribution rising from 12.39% in 2000 to 14.55% in 2020. This increasing impact is primarily attributed to the role of elevation in shaping topography, precipitation patterns, and ecosystem stability. Similarly, annual average temperature showed an upward trend in explanatory ability, increasing from 5.18% in 2000 to 6.81% by 2020. Rising temperatures affect plant growth, alter hydrological conditions and soil properties, and further exacerbate LER.

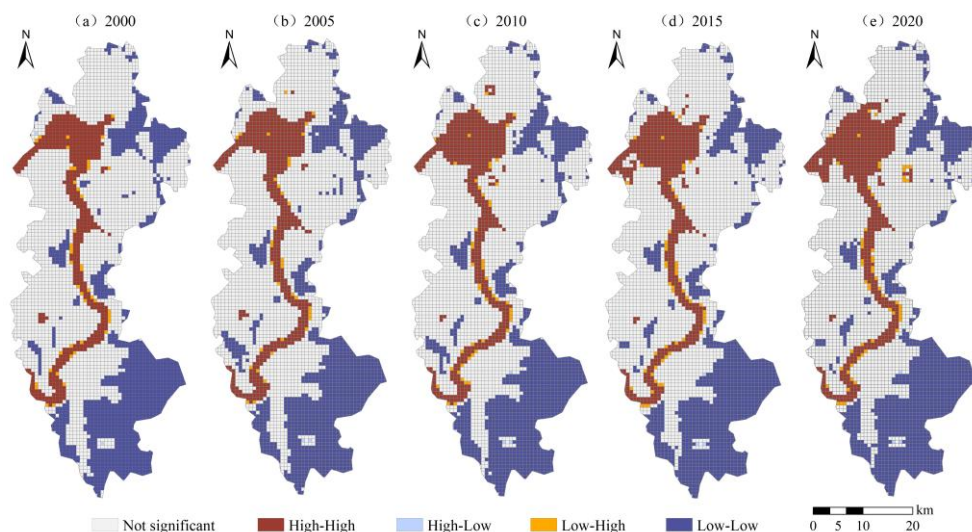


Figure 10. LISA cluster maps of LER in the study area (Zhuzhou City, 2000–2020)

Table 7. Single factor detection results of LER drivers in the study area (Zhuzhou City, 2000–2020)

Driver	Factor	Contribution (%)				
		2000	2005	2010	2015	2020
Natural factor	Elevation	12.39	13.75	13.17	13.64	14.55
	Slope	1.87	2.14	1.87	1.76	1.95
	NDVI	29.08	26.58	22.15	26.72	21.73
	Annual average Temperature	5.18	5.86	5.98	6.39	6.81
	Annual Precipitation	3.44	1.04	1.81	1.17	2.54
	Total contribution	51.95	49.38	44.98	49.67	47.57
Regional accessibility factor	Distance to road	3.82	3.49	3.86	3.10	6.12
	Total contribution	3.82	3.49	3.86	3.10	6.12
Human activity and pollution factor	Population density	8.24	8.88	9.44	8.21	7.05
	Nighttime light	7.46	9.52	9.17	10.67	7.99
	GDP	10.19	9.15	10.97	8.30	6.86
	PM _{2.5} Concentration	10.87	11.57	11.46	11.45	8.94
	Distribution density of key polluting enterprise	1.56	1.50	1.91	2.00	7.65
	SO ₂ Emission	5.89	6.52	8.21	6.59	7.81
	Total contribution	44.22	47.13	51.16	47.22	46.31

Among human activity and pollution factors, PM_{2.5} concentration exhibited the highest explanatory power, with contributions of 10.87%, 11.57%, 11.46%, 11.45%, and 8.94% over the five periods, showing an initial rise before declining. The increase in PM_{2.5} levels is closely linked to urbanization, industrial emissions, and traffic density, underscoring the long-term detrimental effects of air pollution on ecosystems. The contribution of GDP declined from 10.19% in 2000 to 6.86% in 2020 (*Table 7*). Although GDP growth is generally associated with urbanization and economic development, its impact on ecological risk gradually diminished as environmental regulations were strengthened. The contribution of population density declined from 8.24% in 2000 to 7.05% in 2020. The enforcement of sustainable development strategies has effectively alleviated the negative impacts of human activities on LER, particularly in high-density urban areas. The contribution of nighttime light increased from 7.46% in 2000 to 10.67% in 2015 before slightly declining to 7.99% in 2020 (*Table 7*). Despite fluctuations in its contribution, it remains an important influencing factor.

Factor interaction detection

According to *Figure 11*, the top three-factor interactions contributing to LER in 2000 were X3∩X4(0.844), X3∩X7(0.843), and X3∩X5 (0.842). This indicates that the interactions between the NDVI and annual average temperature, annual precipitation, and PM_{2.5} concentration influenced LER evolution to varying degrees. Under humid and warm climatic conditions, precipitation and temperature are critical determinants of vegetation growth and distribution. In contrast, PM_{2.5} concentrations negatively affect air quality and vegetation health, and their interaction exacerbates LER.

In 2005, the strongest interacting factors were X3∩X4 (0.802), X3∩X5 (0.801), and X1∩X3 (0.799). The interactions of NDVI with annual average temperature and annual precipitation remained consistently significant, whereas the interaction between elevation and NDVI highlighted the increasing influence of topography on vegetation distribution, leading to variations in landscape patterns. This variation may be closely linked to local hydrological conditions and the restrictive effects of topography on vegetation growth. By 2010, the most significant interactions were X3∩X4 (0.694), X3∩X10 (0.685), and X2∩X3 (0.672), with an overall decline in interaction strength compared to 2005 (*Fig. 11*). As urbanization and industrial development accelerated, land use changes had an increasing impact on landscape types, making shifts in LER more pronounced. Additionally, the influence of slope on vegetation growth became more significant, particularly in mountainous and sloping areas, where topographic conditions impose greater constraints on vegetation expansion. In 2015, the primary interaction drivers were X3∩X4 (0.798), X2∩X3 (0.781), and X3∩X5 (0.775), all of which showed enhanced interactions compared to 2010 (*Fig. 11*). The most notable increase was observed in the interaction between NDVI and annual precipitation. By 2020, the top three interaction drivers were X3∩X4 (0.691), X3∩X8 (0.687), and X3∩X5 (0.682), with their explanatory power declining compared to the previous period (*Fig. 11*). The NDVI-annual average temperature interaction remained the dominant driver, while NDVI and nighttime light interaction emerged as a major influencing factor for the first time. This shift suggests that as nighttime light intensity increases, the combined effects of land use change and ecological degradation due to urban expansion exert greater stress on vegetation health. These changes lead to significant shifts in landscape types, increased fragmentation and separation, and reduced landscape connectivity, ultimately elevating LER.

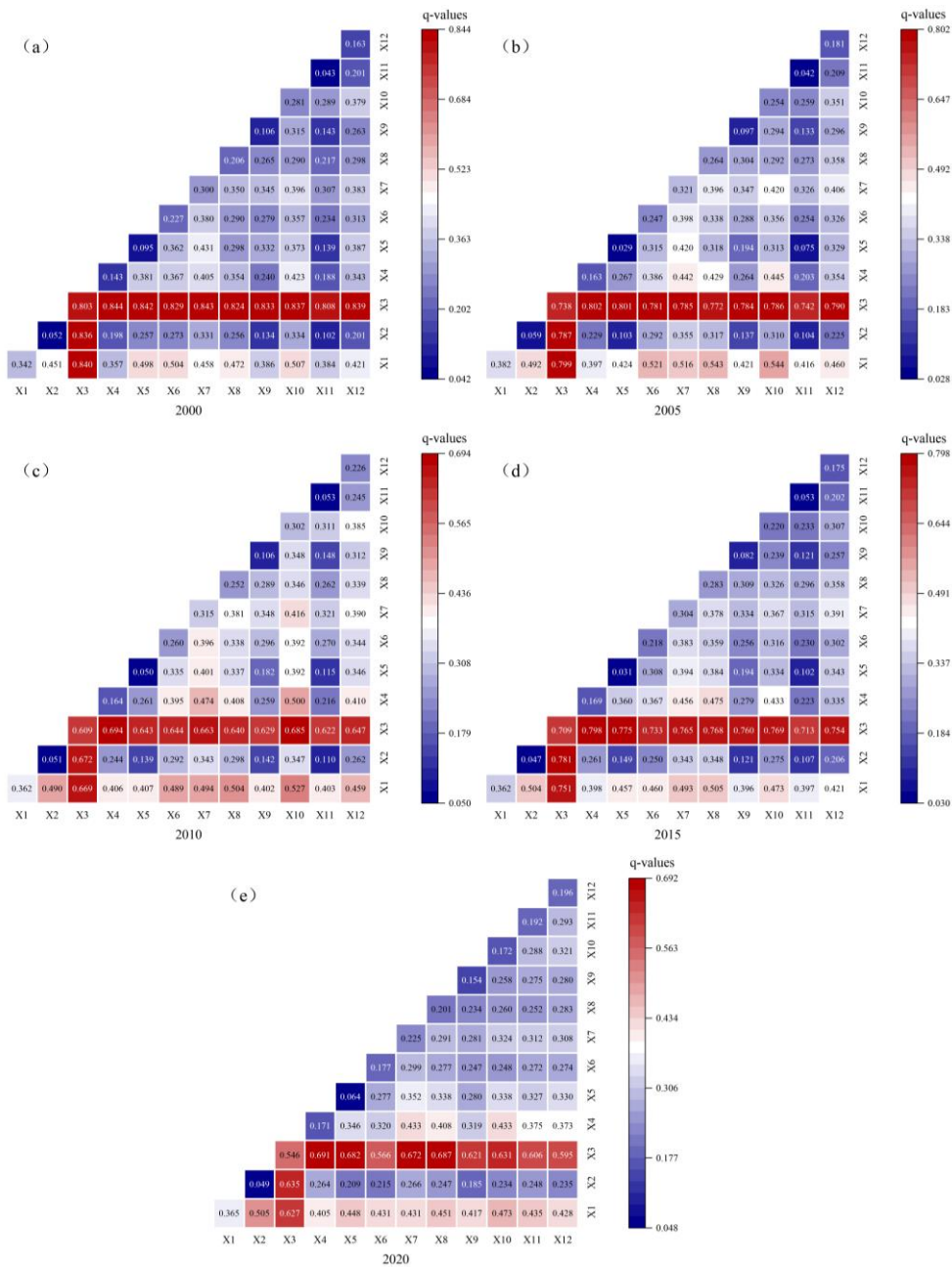


Figure 11. Interaction detection results of LER drivers in the study area (Zhuzhou City, 2000–2020). X1: elevation, X2: slope, X3: NDVI, X4: annual average temperature, X5: annual precipitation, X6: population density, X7: PM_{2.5} concentration, X8: nighttime light, X9: distance to road, X10: GDP, X11: distribution density of key polluting enterprises, X12: SO₂ emissions

Discussion

Causes of land use and landscape pattern changes

Land use and landscape pattern changes can reflect various issues arising from human activities and environmental dynamics. Between 2000 and 2020, Zhuzhou City experienced significant land use transformations, primarily driven by urbanization and economic development. During this period, arable land and construction land expanded

continuously, whereas woodland, grassland, and water exhibited a declining trend. These changes were closely linked to Zhuzhou's policies on urbanization, industrial agglomeration, and ecological protection. Between 2000 and 2020, arable land grew from 740.73 km² to 787.79 km², representing a 6.35% expansion, with the most substantial increase occurring between 2005 and 2010. Notably, construction land expanded significantly, increasing from 65.43 km² to 151.70 km², a 131.86% rise. This trend underscores the rising land demand fueled by urbanization and infrastructure growth, particularly the conversion of arable land and woodland for industrial zone construction and urban growth.

Despite various ecological conservation efforts, including wetland restoration, water conservation, and forest ecological compensation, the area of woodland still declined significantly, decreasing from 1,041.14 km² to 909.50 km², a reduction of 12.64%. This indicates that while ecological protection policies have played a role to some extent, they have not been entirely effective in preventing woodland loss in certain areas amid rapid urbanization. This is closely linked to the strong demand for economic growth and land expansion. Particularly under the pressure of urban expansion, where balancing ecological conservation with economic growth remains a major challenge. Additionally, the grassland area experienced a notable reduction, particularly between 2005 and 2010, shrinking from 1.09 km² to 0.86 km², a 20.61% decrease. This decline largely resulted from the expansion of arable and construction land, which encroached upon natural grassland. In contrast, the water area exhibited only minor changes, decreasing from 69.48 km² in 2000 to 68.03 km² in 2020, a 2.08% decline. The relatively slow rate of change in the water area reflects the reinforcement of wetland conservation policies in recent years, particularly through initiatives such as the Xiangjiang River Basin Water Quality Protection and Wetland Restoration Program, which has been instrumental in mitigating the decline of water resources.

In terms of landscape pattern changes, the fragmentation of arable land has decreased annually, as reflected by a steady increase in LPI, along with improved land connectivity and intensification. These trends indicate agricultural restructuring and enhanced land use efficiency. Conversely, construction land exhibits a clear trend of fragmentation, with increases in both LPI and ED, suggesting that urbanization-driven expansion has led to greater landscape complexity and fragmentation. Although ecological protection measures, such as green corridors and urban greening, have enhanced landscape connectivity to some extent, the continuous expansion of construction land remains a critical concern.

Causes of temporal and spatial changes in LER

Temporally, from 2000 to 2010, low-risk areas constituted the largest proportion of Zhuzhou City, covering nearly half of the total area. However, between 2015 and 2020, medium-low risk areas emerged as the dominant category, occupying more than one-third. The share of medium-risk areas remained relatively stable, while medium-high risk areas constituted a smaller fraction, consistently ranging between 4% and 7%. High-risk areas had the smallest share, fluctuating between 2% and 4% of the total area. From 2000 to 2020, low-risk areas declined significantly, whereas medium-low risk areas exhibited the most substantial expansion. Specifically, the low-risk areas shrank from 848.44 km² in 2000 to 650.31 km² in 2020, reducing by 198.13 km². By contrast, the medium-low risk areas expanded by 192.90 km².

From a spatial perspective, LER changes in Zhuzhou City exhibit a "core improvement, peripheral degradation" dynamic pattern. Between 2000 and 2005, high-risk zones were primarily concentrated in the city center and along the Xiangjiang River Basin, and parts of Lukou District. However, after 2010, high-risk zones in the city center declined significantly, with most of the previously high-risk zones transitioning to medium-high risk levels. The reason is that in the early stages of industrialization, intensive human activities, including excessive land development and occupation, severely disrupted the ecological integrity of urban centers, industrial zones, and transportation hubs, leading to reduced landscape connectivity and heightened ecological risks. However, as urban greening and pollution control measures have been gradually implemented, landscape restoration and ecological remediation projects have started to take effect in certain parts of the urban center, significantly lowering the ecological risk levels in some high-risk zones.

From 2000 to 2020, medium-high risk zones gradually expanded toward the urban periphery, closely linked to industrialization and infrastructure development in suburban areas. In several industrial hubs within Shifeng, Lusong, and Tianyuan Districts, increasing ecological pressures have heightened ecosystem instability. While the proportion of medium-risk zones remained relatively stable, their spatial distribution gradually extended into suburban areas, demonstrating a clear positive correlation between urban expansion and ecological risk. Long-term pollution in the Xiangjiang River Basin has been another critical factor. The accumulation of industrial wastewater, agricultural non-point source pollution, and domestic sewage has resulted in persistent water quality deterioration (Xie et al., 2023), further exacerbating ecological degradation. Water pollution not only intensified aquatic ecological risks but also severely impacted surrounding wetlands and vegetation, contributing to the degradation of previously stable ecosystems. During this period, the Zhuzhou municipal government implemented a series of ecological initiatives, including ecological corridor construction and wetland conservation measures, which facilitated the restoration of certain ecological function zones and constrained the expansion of high-risk and medium-high risk zones. For example, the wetland and ecological restoration project in the Xiangjiang River Basin has improved the river's water quality from Category V to Category IV through wastewater treatment and ecological rehabilitation, with some areas reaching Category III standards (Zhang et al., 2023). This has greatly improved regional ecological stability, thereby reducing ecological risks.

Medium-low risk and low-risk zones are mainly distributed in the northern and southern mountains and remote suburbs of Zhuzhou, as well as in nature reserves situated far from urban centers. These regions experience moderate levels of human disturbance, feature high terrain and dense vegetation, and are dominated by natural landscapes with relatively low development pressure, allowing them to maintain a relatively stable ecological environment, thereby exhibiting low LER. However, with the expansion of infrastructure and increasing human activities, some low-risk zones have gradually transitioned into medium-low risk zones, particularly in the central region of the study area and mountainous areas. This transformation is mainly driven by urbanization-induced land use changes, road construction, and agricultural expansion, which have disrupted the original natural landscape, reduced ecosystem stability, and weakened ecological functions. Therefore, it is essential to improve continuous monitoring of ecological quality in these areas, focusing on key indicators such as water quality,

vegetation cover, and ecosystem service functions to identify potential risks early and prevent large-scale LER deterioration.

The study results indicate that between 2000 and 2020, the dominant trend in LER transitions involved low-risk areas shifting into medium-low risk, medium-risk transitioning into medium-low risk, medium-high risk converting into medium-risk, and high-risk transforming into medium-high risk areas. Notably, since 2014, some low-risk zones have progressively evolved into ecologically stable areas, while certain high-risk zones—such as the Xiangjiang River Basin and industrial zones—have undergone effective restoration, reducing ecological risks. This pattern is particularly evident in Shifeng District, where the extent of medium-high risk zones initially expanded northwestward before later contracting. For instance, Qingshuitang, historically one of Zhuzhou's most polluted industrial zones, suffered severe soil acidification, vegetation degradation, and soil erosion due to prolonged industrial activity (Shen et al., 2018), resulting in a continuous rise in LER. However, with the launch of industrial relocation efforts in 2014, and the full shutdown of industrial operations in 2018, remediation efforts significantly improved environmental conditions. Consequently, the extent of medium-high risk zones in Shifeng District gradually contracted, leading to improved ecological stability.

Comprehensive analysis of LER driving factors

Findings from single-factor detection reveal that among natural factors, NDVI and elevation are the key factors influencing LER, with a combined contribution exceeding 41%. This finding differs from the conclusions of Gao et al. (2024), who identified anthropogenic disturbances as the dominant drivers of LER. The discrepancy may stem from differences in study areas and temporal scales. NDVI played a leading role in LER evolution, consistently contributing over 20%. As a key indicator of vegetation coverage and growth status, NDVI effectively reflects the impact of vegetation dynamics on LER (Xu et al., 2020). Its sustained dominance may be closely related to the spatial distribution of vegetation cover and seasonal growth variations. This effect becomes particularly pronounced during periods of precipitation and temperature fluctuations, further amplifying its role in LER evolution. The contribution of elevation increased annually, fluctuating between 12% and 15%. Elevation is a critical topographic indicator that directly affects ecological vulnerability. Its interaction with annual precipitation further amplifies its impact on LER. Additionally, the contribution of annual average temperature continued to increase, indicating that rising temperatures exacerbate ecological stress, making temperature fluctuations an increasingly critical factor affecting landscape ecosystems. Meanwhile, the influence of the regional accessibility factor on LER evolution remained relatively stable but showed an upward trend.

With respect to human activity and pollution factors, PM_{2.5} concentration, GDP, nighttime light, and population density had the greatest impact on LER. The contribution of PM_{2.5} concentration rose from 10.87% in 2000 to 11.57% in 2010 before slightly declining in subsequent years. However, it remained the most dominant driver of LER. This trend suggests that air pollution control measures in Zhuzhou City have yielded initial results, PM_{2.5} concentration has declined. Nevertheless, the long-term impact of industrial emissions and pollution remains profound. This is consistent with the conclusions of Li et al. (2016), who suggested that PM_{2.5} concentration is strongly linked to urbanization and industrial emissions. The escalation of PM_{2.5} levels has exacerbated ecological risks, particularly in heavily polluted areas, where air pollution poses a serious

threat to ecosystem stability. PM_{2.5} concentration can influence landscape ecological risk by impairing vegetation growth, altering microclimates, and degrading habitat quality—factors that in turn affect the spatial configuration of land use. Empirical studies in China have shown that PM_{2.5} pollution delays spring green-up, suppresses photosynthesis, and reduces carbon uptake, thereby weakening vegetation structure and altering NDVI dynamics. These ecological disruptions can offset climate-driven improvements in vegetation conditions (Qu et al., 2025), ultimately reshaping land use patterns through feedbacks on ecosystem services and land cover viability. Although PM_{2.5} levels may also be affected by land use activities, its strong spatial association with environmental stress and urban–industrial intensity supports its role as a proxy indicator in ecological risk analysis. Therefore, while strict causality remains difficult to establish, the convergence of documented ecological impacts and robust statistical associations justifies its inclusion as a driver variable in this study. GDP, nighttime light, and population density primarily reflect the expansion of economic activities and urbanization. With the implementation of green development strategies, the impact of economic growth on ecological risk has gradually weakened. Economic development no longer unilaterally drives an increase in ecological risk but has, in some areas, contributed to risk mitigation. Population density directly reflects the intensity of human disturbance. Typically, higher density correlates with increased ecological risk. However, ecological protection policies and land-use planning have effectively mitigated the negative impacts of population growth on LER. From an overall perspective, natural factors remain the dominant drivers of LER's spatial evolution; human activity and pollution factors have increasingly emerged as key drivers of rising ecological risk. The findings further confirm the multifaceted impact of human activities on LER, particularly the long-term ecological pressure exerted by air pollution, population density, and economic activities, which significantly shape changes in ecological risk.

The interaction detection results revealed that all factor interactions demonstrated either bivariate enhancement or nonlinear enhancement effects, suggesting synergistic effects far exceeding individual factor influences on LER. The q -values of $X3 \cap X1 \sim X12$ and $X1 \cap X2 \sim X12$ were consistently high, suggesting that the interactions between NDVI, elevation, and other factors were the primary driving forces behind LER evolution in Zhuzhou City. These findings differ from those of Chen et al. (2024), who suggested that human disturbance and land use intensity play a more dominant role in shaping LER dynamics. This discrepancy may be attributed to differences in geographical context and the selected driving factors.

Firstly, the significant interaction between NDVI and elevation ($X1$) and slope ($X2$) suggests that topographic factors play a crucial role in determining vegetation distribution and ecosystem stability. Elevation influences temperature, humidity, and soil moisture availability, thereby affecting plant growth, while slope regulates water loss and soil erosion processes, further impacting vegetation cover. Additionally, the strong interaction between NDVI and mean annual temperature ($X4$) as well as annual precipitation ($X5$) indicates that the direct impacts of climate change on vegetation growth cannot be overlooked in the evolution of ecological risk. Warmer and more humid climates generally promote vegetation growth, whereas climatic extremes, such as prolonged droughts or heavy rainfall, contribute to vegetation degradation. This climate-vegetation interaction exacerbates spatial disparities in LER.

Secondly, the strong interactions between NDVI and PM_{2.5} concentration ($X7$) and SO₂ emissions ($X12$) reflect the adverse effects of atmospheric pollution on vegetation

growth, as pollutant deposition can impair leaf photosynthesis and negatively impact plant health. Additionally, the interactions between NDVI and nighttime light (X8), population density (X6), and GDP (X10) suggest that urbanization and economic development exert profound influences on vegetation growth by altering land use patterns, increasing infrastructure construction, and intensifying anthropogenic pollution emissions. For instance, urban expansion is typically associated with vegetation loss, whereas urban greening initiatives may help mitigate ecological risks to some extent. Thus, NDVI dynamics are influenced not only by natural factors but also by the complex interplay of urbanization processes and pollution levels.

Moreover, the study revealed that although the explanatory power of the distribution density of key polluting enterprise (X11) and distance to road (X9) was relatively low in single-factor detection, their *q*-values increased significantly when interacting with NDVI, highest exceeding 0.8 in both cases. This suggests that while the spatial distribution of pollution sources and transportation networks may have a limited direct impact on vegetation when considered independently, their influence becomes significantly amplified when vegetation functions as an ecological buffer. Through its ability to absorb, retain, and disperse pollutants, vegetation enhances the cumulative effects of these factors, further highlighting the indirect role of pollution sources in driving LER. For instance, roadside vegetation is not only directly affected by vehicle exhaust emissions and dust accumulation but also suffers from such as soil contamination, noise pollution, and physical disturbance, all of which contribute to ecological degradation and an elevated LER. NDVI values tend to be lower near roads, reflecting the destructive impact of road construction and increased human activity on vegetation cover. Conversely, areas farther from roads generally exhibit higher vegetation recovery capacity. The study also identified that the interaction between annual precipitation (X5) and PM_{2.5} concentration (X7) was particularly evident, demonstrating the synergistic effects of atmospheric pollution and hydrological processes on ecological risk. Precipitation facilitates the wet deposition of PM_{2.5}, reducing its concentration in the atmosphere; however, excessive precipitation can lead to soil erosion, vegetation root scouring, and further alterations in ecosystem structure. Consequently, in years with higher precipitation, the impact of PM_{2.5} pollution on LER may be relatively mitigated, whereas, in drier years, the cumulative effects of pollution could pose a greater threat to vegetation health.

Finally, the interaction between elevation and socio-economic factors such as GDP, PM_{2.5} concentration, nighttime light, and population density is also one of the major contributors to LER changes in Zhuzhou City. In low-elevation areas, higher development density intensifies ecological pressure, whereas high-elevation areas, despite lower development density, exhibit greater ecological vulnerability. As a result, the rise of GDP, nighttime lighting, population density, and PM_{2.5} concentration further deteriorates these already fragile ecosystems, exacerbating LER. Furthermore, the limitations of transportation and infrastructure in high-elevation areas amplify the ecological consequences of economic expansion, making urbanization's impact in these regions even more pronounced.

Overall, NDVI exhibits high explanatory power in multi-factor interactions due to its dual responsiveness to both natural environmental conditions and anthropogenic activities. Vegetation cover changes are not only directly regulated by natural factors including topography and climate but are also indirectly influenced by urbanization, pollution emissions, and infrastructure development. NDVI can be considered as a key

regulatory factor in LER, with its synergistic interactions with other driving factors further intensifying its spatial heterogeneity. Therefore, effective landscape ecological management and risk mitigation require a comprehensively assessment the synergistic effects of natural factors and anthropogenic influences on vegetation, enabling the development of more targeted ecological protection measures and sustainable development strategies.

Conclusions

This research provided an in-depth examination of the spatiotemporal evolution of land use, landscape patterns, and LER in Zhuzhou City from 2000 to 2020. Additionally, the key drivers of LER were identified using the Geodetector method. The key findings are as follows:

(1) Between 2000 and 2020, land use changes in Zhuzhou City were primarily characterized by expanded arable and construction land, alongside reduced woodland, grassland, and water. Construction land exhibited the highest fluctuation in land use dynamics, with the most pronounced changes occurring between 2005 and 2010. Land use transitions mainly occurred between woodland and arable land, with woodland being converted to arable land and construction land, whereas arable land was converted into both woodland and construction land.

(2) The fragmentation of arable land in Zhuzhou City decreased over time, with patches becoming more concentrated and the dominance of the largest patches increasing. The fragmentation of woodland patches showed signs of slowing, whereas the fragmentation of construction land intensified, exhibiting a strong landscape agglomeration effect. The dominance of water was threatened during urbanization but showed signs of recovery following the adoption of ecological protection measures. The spatial configuration of construction land became increasingly complex, with greater edge irregularity. Overall, landscape fragmentation in Zhuzhou City increased annually with urban expansion; however, ecological protection policies enhanced landscape connectivity. Meanwhile, landscape diversity steadily increased, increasing ecosystem complexity and richness.

(3) Low-risk and medium-low risk areas predominate in Zhuzhou City, collectively covering over 70% of the total area. The low-risk area has gradually declined over the years, primarily transitioning into medium-low risk areas. Similarly, medium-risk and high-risk areas have decreased in area, with most of their transitions occurring toward medium-low and medium-high risk areas. The spatial distribution of LER in Zhuzhou City has become more concentrated, with an overall expansion of medium-low and medium-high risk zones. High-risk zones are primarily concentrated in the city centre and along the Xiangjiang River Basin, though the overall risk level has decreased significantly. Lower-risk zones, characterized by healthier ecological conditions and minimal human disturbance, are primarily distributed in nature reserves and mountainous regions far from the urban core. Spatial autocorrelation analysis confirms that the LER in Zhuzhou City exhibits strong positive spatial correlation, with distinct "High-High" and "Low-Low" clustering.

(4) More than 75% of the region's LER levels remained unchanged. Zhuzhou's landscape ecosystem has undergone a trajectory of deterioration—significant deterioration—sustained local deterioration—overall improvement, yet the overall LER level has slightly increased, a decline in ecosystem stability. The spatial pattern of LER

in Zhuzhou City generally follows a “core improvement, peripheral deterioration” trend. Risk decrease zones are primarily concentrated in the urban core, southwestern Tianyuan District, and northern Shifeng District, mainly influenced by policy interventions. In contrast, risk increase zones are most evident in Tianyuan, Lusong, and Hetang Districts, where industrialization and urbanization have heightened ecological instability.

(5) The evolution of LER in Zhuzhou City is jointly driven by natural environmental conditions, human activities, and pollution levels, with significant interaction effects. Single-factor detection results indicate that NDVI, elevation, PM_{2.5} concentration, GDP, nighttime light, and population density are the dominant influencing factors of LER. The interaction detection results consistently exhibited enhancement, with NDVI and elevation showing high q-values after interacting with other factors. Specifically, the interactions of NDVI with annual average temperature, PM_{2.5} concentration, and annual precipitation exerted the most pronounced influence on LER.

Author contributions. Yi Hanlin: Conceptualization, Methodology, Data curation, Software, Validation, Formal analysis, Investigation, Visualization, Writing—original draft preparation, Writing—review & editing. Zhu Jiayi: Writing—review & editing.

Acknowledgements. The authors sincerely appreciate the constructive comments and suggestions provided by the editor and anonymous reviewers.

Conflicts of interest. The authors declare no conflicts of interest.

REFERENCES

- [1] Albert, C. H., Hervé, M., Fader, M., Bondeau, A., Leriche, A., Monnet, A.-C., Cramer, W. (2020): What ecologists should know before using land use/cover change projections for biodiversity and ecosystem service assessments. – *Regional Environmental Change* 20: 106. <https://doi.org/10.1007/s10113-020-01675-w>
- [2] Aruhan, Liu, D. C. (2024): Study on the influencing factors of the evolution of space pattern based on principal component analysis in Duolun County. – *Scientific Reports* 14: 20567.
- [3] Cao, Q., Zhang, X., Lei, D., Guo, L., Sun, X., Wu, J. (2019): Multi-scenario simulation of landscape ecological risk probability to facilitate different decision-making preferences. – *Journal of Cleaner Production* 227: 325-335.
- [4] Chang, X., Xing, Y., Gong, W., Yang, C., Guo, Z., Wang, D., Wang, J., Yang, H., Xue, G., Yang, S. (2023): Evaluating gross primary productivity over 9 ChinaFlux sites based on random forest regression models, remote sensing, and eddy covariance data. – *Science of the Total Environment* 875: 162601.
- [5] Chen, H., Liu, J., Cao, Y., Li, S., Ouyang, H. (2006): Progresses of ecological risk assessment. – *Acta Ecologica Sinica* 26: 1558-1566.
- [6] Chen, S., Chen, B., Fath, B. D. (2013): Ecological risk assessment on the system scale: a review of state-of-the-art models and future perspectives. – *Ecological Modelling* 250: 25-33.
- [7] Chen, J., Dong, B., Li, H., Zhang, S., Peng, L., Fang, L., Zhang, C., Li, S. (2020): Study on landscape ecological risk assessment of Hooded Crane breeding and overwintering habitat. – *Environmental Research* 187: 109649.
- [8] Chen, H., Chen, H., Huang, X., Zhang, S., He, T., Gao, Z. (2024): Landscape ecological risk assessment and driving factor analysis in southwest China. – *Scientific Reports* 14: 23208.

- [9] Cheng, X., Zhang, Y., Yang, G., Nie, W., Wang, Y., Wang, J., Xu, B. (2023): Landscape ecological risk assessment and influencing factor analysis of basins in suburban areas of large cities—A case study of the Fuchunjiang River Basin, China. – *Frontiers in Ecology and Evolution* 11: 1184273.
- [10] Chu, L., Sun, T., Wang, T., Li, Z., Cai, C. (2018): Evolution and prediction of landscape pattern and habitat quality based on CA-Markov and InVEST model in Hubei section of Three Gorges Reservoir Area (TGRA). – *Sustainability* 10: 3854.
- [11] Deng, R., Ding, X., Wang, J. (2023): Landscape ecological risk assessment and spatial pattern evolution analysis of the Central Yunnan Urban Agglomeration from 1995 to 2020 based on land use/cover change. – *Sustainability* 15: 16641.
- [12] Du, L., Dong, C., Kang, X., Qian, X., Gu, L. (2023): Spatiotemporal evolution of land cover changes and landscape ecological risk assessment in the Yellow River Basin, 2015-2020. – *Journal of Environmental Management* 332: 117149.
- [13] Fan, J., Wang, Y., Zhou, Z., You, N., Meng, J. (2016): Dynamic ecological risk assessment and management of land use in the middle reaches of the Heihe River based on landscape patterns and spatial statistics. – *Sustainability* 8: 536.
- [14] Foley, J. A., DeFries, R., Asner, G. P., Barford, C., Bonan, G., Carpenter, S. R., Chapin, F. S., Coe, M. T., Daily, G. C., Gibbs, H. K. (2005): Global consequences of land use. – *Science* 309: 570-574.
- [15] Gao, L., Zhao, Z., Song, D., Pei, X. (2024): Evolution of landscape ecological risk and its response to natural and anthropogenic factors: A case study of ecological conservation area in Beijing. – *China Environmental Science* 44: 4032-4041.
- [16] Gong, J., Cao, E., Xie, Y., Xu, C., Li, H., Yan, L. (2021): Integrating ecosystem services and landscape ecological risk into adaptive management: Insights from a western mountain-basin area, China. – *Journal of Environmental Management* 281: 111817.
- [17] Grimm, N. B., Faeth, S. H., Golubiewski, N. E., Redman, C. L., Wu, J., Bai, X., Briggs, J. M. (2008): Global change and the ecology of cities. – *Science* 319: 756-760.
- [18] Haque, M. R., Ali, M. M., Ahmed, W., Rahman, M. M. (2022): Assessment of metal (loid) s pollution in water and sediment from an urban river in Bangladesh: An ecological and health risk appraisals. – *Case Studies in Chemical and Environmental Engineering* 6: 100272.
- [19] Harwell, M. A., Cooper, W., Flaak, R. (1992): Prioritizing ecological and human welfare risks from environmental stresses. – *Environmental Management* 16: 451-464.
- [20] Hou, M., Ge, J., Gao, J., Meng, B., Li, Y., Yin, J., Liu, J., Feng, Q., Liang, T. (2020): Ecological risk assessment and impact factor analysis of alpine wetland ecosystem based on LUCC and boosted regression tree on the Zoige Plateau, China. – *Remote Sensing* 12: 368.
- [21] How, C. M., Kuo, Y.-H., Huang, M.-L., Liao, V. H.-C. (2023): Assessing the ecological risk and ecotoxicity of the microbially mediated restoration of heavy metal-contaminated river sediment. – *Science of the Total Environment* 858: 159732.
- [22] Hu, A. (2018): Ecological civilization construction and green development. – In: Hu, A. (ed.) *China's Road and China's Dream: An Analysis of the Chinese Political Decision-Making Process Through the National Party Congress*. Springer, Singapore.
- [23] Ji, Y., Bai, Z., Hui, J. (2021): Landscape ecological risk assessment based on LUCC-A case study of Chaoyang county, China. – *Forests* 12: 1157.
- [24] Kadoya, T., Washitani, I. (2011): The Satoyama Index: A biodiversity indicator for agricultural landscapes. – *Agriculture, Ecosystems & Environment* 140: 20-26.
- [25] Ke, X., Wang, X., Guo, H., Yang, C., Zhou, Q., Mougharbel, A. (2021): Urban ecological security evaluation and spatial correlation research-based on data analysis of 16 cities in Hubei Province of China. – *Journal of Cleaner Production* 311: 127613.
- [26] Lee, B. X., Kjaerulf, F., Turner, S., Cohen, L., Donnelly, P. D., Muggah, R., Davis, R., Realini, A., Kieselbach, B., MacGregor, L. S. (2016): *Transforming our world:*

- implementing the 2030 agenda through sustainable development goal indicators. – *Journal of Public Health Policy* 37: 13-31.
- [27] Li, G., Fang, C., Wang, S., Sun, S. (2016): The effect of economic growth, urbanization, and industrialization on fine particulate matter (PM_{2.5}) concentrations in China. – *Environmental Science & Technology* 50: 11452-11459.
- [28] Li, Z., Jiang, W., Wang, W., Chen, Z., Ling, Z., Lv, J. (2020): Ecological risk assessment of the wetlands in Beijing-Tianjin-Hebei urban agglomeration. – *Ecological Indicators* 117: 106677.
- [29] Li, L., Zhou, X., Yang, L., Duan, J., Zeng, Z. (2022): Spatio-temporal characteristics and influencing factors of ecological risk in China's north-south transition zone. – *Sustainability* 14: 5464.
- [30] Li, B., Yang, Y., Jiao, L., Yang, M., Li, T. (2023): Selecting ecologically appropriate scales to assess landscape ecological risk in megacity Beijing, China. – *Ecological Indicators* 154: 110780.
- [31] Lin, Z., Peng, S., Pu, S., Ma, X., Zhou, Y. (2020): Landscape ecological risk assessment of Dianchi Lake Basin based on land use change. – *IOP Conference Series: Materials Science and Engineering* 730: 012033.
- [32] Liu, Y., Li, T., Zhao, W., Wang, S., Fu, B. (2019): Landscape functional zoning at a county level based on ecosystem services bundle: Methods comparison and management indication. – *Journal of Environmental Management* 249: 109315.
- [33] Liu, Y., Wu, K., Cao, H. (2022): Land-use change and its driving factors in Henan province from 1995 to 2015. – *Arabian Journal of Geosciences* 15: 247.
- [34] Long, X., Lin, H., An, X., Chen, S., Qi, S., Zhang, M. (2022): Evaluation and analysis of ecosystem service value based on land use/cover change in Dongting Lake wetland. – *Ecological Indicators* 136: 108619.
- [35] Lu, Y., Yang, X., Bian, D., Chen, Y., Li, Y., Yuan, Z., Wang, K. (2023): A novel approach for quantifying water resource spatial equilibrium based on the regional evaluation, spatiotemporal heterogeneity and geodetector analysis integrated model. – *Journal of Cleaner Production* 424: 138791.
- [36] Malekmohammadi, B., Blouchi, L. R. (2014): Ecological risk assessment of wetland ecosystems using multi criteria decision making and geographic information system. – *Ecological Indicators* 41: 133-144.
- [37] Mo, W., Wang, Y., Zhang, Y., Zhuang, D. (2017): Impacts of road network expansion on landscape ecological risk in a megacity, China: A case study of Beijing. – *Science of the Total Environment* 574: 1000-1011.
- [38] Mondal, B., Sharma, P., Kundu, D., Bansal, S. (2021): Spatio-temporal assessment of landscape ecological risk and associated drivers: A case study of Delhi. – *Environment and Urbanization Asia* 12: S85-S106.
- [39] Pătru-Stupariu, I., Nita, A. (2022): Impacts of the European Landscape Convention on interdisciplinary and transdisciplinary research. – *Landscape Ecology* 37: 1211-1225.
- [40] Peng, Y., Welden, N., Renaud, F. G. (2023): A framework for integrating ecosystem services indicators into vulnerability and risk assessments of deltaic social-ecological systems. – *Journal of Environmental Management* 326: 116682.
- [41] Qu, W., Hua, H., Yang, T., Zohner, C. M., Peñuelas, J., Wei, J., Yu, L., Wu, C. (2025): Delayed leaf green-up is associated with fine particulate air pollution in China. – *Nature Communications* 16: 3406.
- [42] Ran, P., Hu, S., Frazier, A. E., Qu, S., Yu, D., Tong, L. (2022): Exploring changes in landscape ecological risk in the Yangtze River Economic Belt from a spatiotemporal perspective. – *Ecological Indicators* 137: 108744.
- [43] Rao, J., Ouyang, X., Pan, P., Huang, C., Li, J., Ye, Q. (2024): Ecological Risk Assessment of Forest Landscapes in Lushan National Nature Reserve in Jiangxi Province, China. – *Forests* 15: 484.

- [44] Setiyoko, A., Basaruddin, T., Arymurthy, A. M. (2020): Minimax approach for semivariogram fitting in ordinary kriging. – *IEEE Access* 8: 82054-82065.
- [45] Shen, L., Li, Z.-H., Zeng, W.-M., Yu, R.-L., Wu, X.-L., Li, J.-K., Wang, S.-K. (2018): Microbial communities in soils of Qingshuitang industrial district in Zhuzhou. – *Environmental Science* 39: 5151-5162.
- [46] Shi, Y., Feng, C.-C., Yu, Q., Han, R., Guo, L. (2022): Contradiction or coordination? The spatiotemporal relationship between landscape ecological risks and urbanization from coupling perspectives in China. – *Journal of Cleaner Production* 363: 132557.
- [47] Shi, H., Wang, P., Zheng, J., Deng, Y., Zhuang, C., Huang, F., Xiao, R. (2023): A comprehensive framework for identifying contributing factors of soil trace metal pollution using Geodetector and spatial bivariate analysis. – *Science of the Total Environment* 857: 159636.
- [48] Stupariu, M.-S., Cushman, S. A., Pleşoiianu, A.-I., Pătru-Stupariu, I., Fuerst, C. (2022): Machine learning in landscape ecological analysis: a review of recent approaches. – *Landscape Ecology* 37: 1227-1250.
- [49] Tan, L., Luo, W., Yang, B., Huang, M., Shuai, S., Cheng, C., Zhou, X., Li, M., Hu, C. (2023): Evaluation of landscape ecological risk in key ecological functional zone of South-to-North Water Diversion Project, China. – *Ecological Indicators* 147: 109934.
- [50] Turner, B. L., Lambin, E. F., Reenberg, A. (2007): The emergence of land change science for global environmental change and sustainability. – *Proceedings of the National Academy of Sciences* 104: 20666-20671.
- [51] Wang, J., Xu, C. (2017): Geodetector: Principle and prospective. – *Acta Geographica Sinica* 72: 116-134.
- [52] Wang, Z.-B., Li, J.-X., Liang, L.-W. (2020): Spatio-temporal evolution of ozone pollution and its influencing factors in the Beijing-Tianjin-Hebei Urban Agglomeration. – *Environmental Pollution* 256: 113419.
- [53] Wang, H., Liu, X., Zhao, C., Chang, Y., Liu, Y., Zang, F. (2021): Spatial-temporal pattern analysis of landscape ecological risk assessment based on land use/land cover change in Baishuijiang National nature reserve in Gansu Province, China. – *Ecological Indicators* 124: 107454.
- [54] Wang, X., Zhu, T., Jiang, C. (2025): Landscape ecological risk based on optimal scale and its tradeoff/synergy with human activities: A case study of the Nanjing metropolitan area, China. – *Ecological Indicators* 170: 113040.
- [55] Wei, J., Li, Z., Lyapustin, A., Sun, L., Peng, Y., Xue, W., Su, T., Cribb, M. (2021): Reconstructing 1-km-resolution high-quality PM_{2.5} data records from 2000 to 2018 in China: spatiotemporal variations and policy implications. – *Remote Sensing of Environment* 252: 112136.
- [56] Wu, J., Zhu, Q., Qiao, N., Wang, Z., Sha, W., Luo, K., Wang, H., Feng, Z. (2021): Ecological risk assessment of coal mine area based on “source-sink” landscape theory—A case study of Pingshuo mining area. – *Journal of Cleaner Production* 295: 126371.
- [57] Xie, H., He, Y., Choi, Y., Chen, Q., Cheng, H. (2020): Warning of negative effects of land-use changes on ecological security based on GIS. – *Science of the Total Environment* 704: 135427.
- [58] Xie, H., Wen, J., Chen, Q., Wu, Q. (2021): Evaluating the landscape ecological risk based on GIS: A case-study in the poyang lake region of China. – *Land Degradation & Development* 32: 2762-2774.
- [59] Xie, Y., Zhao, Y., Zhang, Q., Yu, H., Zhou, Y., Zhou, P., Li, F., Xiong, H. (2023): Analysis of impact and causes on protection and treatment on water quality of Xiangjiang River. – *Research of Agricultural Modernization* 44: 173-183.
- [60] Xu, Y., Xu, X., Tang, Q. (2016): Human activity intensity of land surface: Concept, methods and application in China. – *Journal of Geographical Sciences* 26: 1349-1361.

- [61] Xu, X., Jiang, H., Guan, M., Wang, L., Huang, Y., Jiang, Y., Wang, A. (2020): Vegetation responses to extreme climatic indices in coastal China from 1986 to 2015. – *Science of the Total Environment* 744: 140784.
- [62] Xu, M., Bao, C. (2022): Quantifying the spatiotemporal characteristics of China's energy efficiency and its driving factors: A Super-RSBM and Geodetector analysis. – *Journal of Cleaner Production* 356: 131867.
- [63] Yang, J., Huang, X. (2021): 30 m annual land cover and its dynamics in China from 1990 to 2019. – *Earth System Science Data Discussions* 2021: 1-29.
- [64] Yang, L. A., Li, Y., Jia, L., Ji, Y., Hu, G. (2023): Ecological risk assessment and ecological security pattern optimization in the middle reaches of the Yellow River based on ERI+MCR model. – *Journal of Geographical Sciences* 33: 823-844.
- [65] Yuan, Y., Cave, M., Xu, H., Zhang, C. (2020): Exploration of spatially varying relationships between Pb and Al in urban soils of London at the regional scale using geographically weighted regression (GWR). – *Journal of Hazardous materials* 393: 122377.
- [66] Zhang, X., Yao, L., Luo, J., Liang, W. (2022): Exploring changes in land use and landscape ecological risk in key regions of the belt and road initiative countries. – *Land* 11: 940.
- [67] Zhang, Y., Yi, L., Xie, B., Li, J., Xiao, J., Xie, J., Liu, Z. (2023): Analysis of ecological quality changes and influencing factors in Xiangjiang River Basin. – *Scientific Reports* 13: 4375.
- [68] Zhang, S. H., Jiang, H. L., Yu, H. L., Feng, X. H. (2024): Spatio-temporal Evolution and Driving Force Analysis of Landscape Ecological Risk in Shenyang Modern Metropolitan. – *Ecology and Environment* 33: 1471.
- [69] Zheng, K., Tan, L., Sun, Y., Wu, Y., Duan, Z., Xu, Y., Gao, C. (2021): Impacts of climate change and anthropogenic activities on vegetation change: Evidence from typical areas in China. – *Ecological Indicators* 126: 107648.
- [70] Zhuo, J., Zhai, D. Q., Mao, Y. Y. (2024): Analysis of Spatiotemporal Evolution of Landscape Ecological Risk in the Fujian Delta Urban Agglomeration. – *Landscape Architecture* 31: 111-119.